December 2003 • NREL/CP-500-35090

Conference Paper

Wind Tunnel Aeroacoustic Tests of Six Airfoils for Use on Small Wind Turbines

Preprint

P. Migliore
National Renewable Energy Laboratory

S. Oerlemans
National Aerospace Laboratory
NLR Department of Aeroacoustics

To be presented at the 2004 AIAA Wind Energy Symposium
Reno, Nevada
January 5–8, 2004

National Renewable Energy Laboratory

1617 Cole Boulevard
Golden, Colorado 80401-3393

NREL is a U.S. Department of Energy Laboratory
Operated by Midwest Research Institute • Battelle

Contract No. DE-AC36-99-GO10337

WIND TUNNEL AEROACOUSTIC TESTS OF SIX AIRFOILS FOR USE ON SMALL WIND TURBINES[*§]

Paul Migliore
National Renewable Energy Laboratory, National Wind Technology Center
1617 Cole Boulevard, Golden, Colorado 80401, USA
paul_migliore@nrel.gov

Stefan Oerlemans
National Aerospace Laboratory NLR, Department of Aeroacoustics
P.O. Box 153, 8300 AD Emmeloord, The Netherlands
stefan@nlr.nl

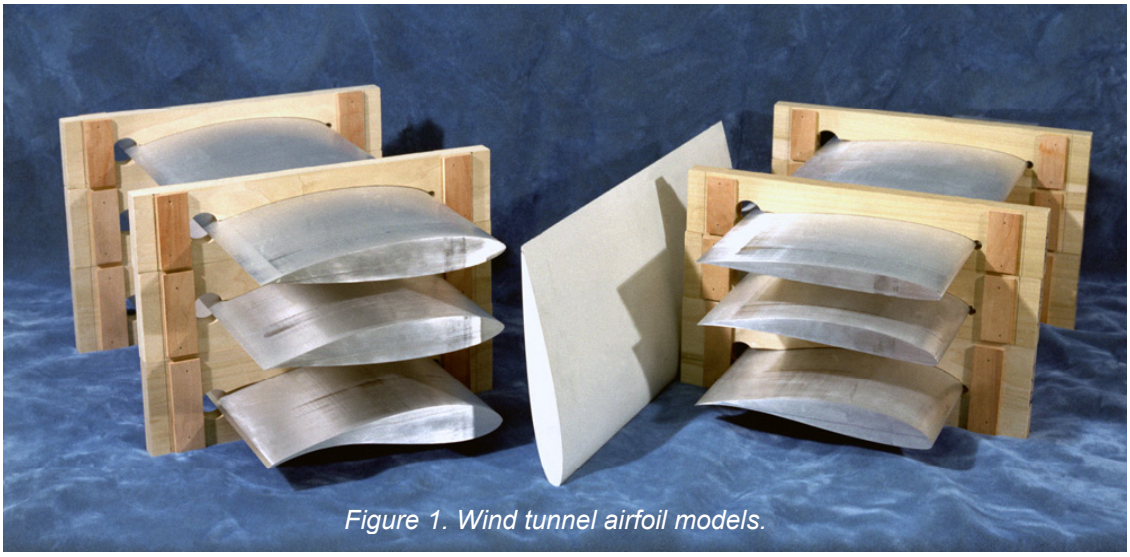

Figure 1. Wind tunnel airfoil models.

ABSTRACT

Aeroacoustic tests of seven airfoils were performed in an open jet anechoic wind tunnel. Six of the airfoils are candidates for use on small wind turbines operating at low Reynolds number. One airfoil was tested for comparison to benchmark data. Tests were conducted with and without boundary layer tripping. In some cases a turbulence grid was placed upstream in the test section to investigate inflow turbulence noise. An array of 48 microphones was used to locate noise sources and separate airfoil noise from extraneous tunnel noise. Trailing edge noise was dominant for all airfoils in clean tunnel flow. With the boundary layer untripped, several airfoils exhibited pure tones that disappeared after proper tripping was applied. In the presence of inflow turbulence, leading edge noise was dominant for all airfoils.

INTRODUCTION

The U.S. Department of Energy, working through its National Renewable Energy Laboratory (NREL), is engaged in a comprehensive research effort to improve the understanding of wind turbine aeroacoustics. The research is motivated by the desire to make use of the large expanse of low wind speed sites that tend to be closer to U.S. load centers. Quiet wind turbines are an inducement to widespread deployment, so the goal of NREL's aeroacoustic research is to develop tools for use by U.S. industry in developing highly efficient, quiet wind turbines for deployment at these low wind speed sites. NREL's National Wind Technology Center (NWTC) is implementing a multi-faceted research approach that includes wind tunnel tests, field tests and theoretical analyses in direct support of low wind speed turbine development by its industry partners. NWTC researchers are working hand-in-hand with industry engineers to ensure that research findings are available to support ongoing design decisions.

[*] This work was performed at the National Renewable Energy Laboratory in support of the U.S. Department of Energy under Contract No. DE-AC36-99GO10337.

The work described herein focuses on the experimental aeroacoustic analysis of six airfoils that are candidates for use on small wind turbines. However, without knowledge of both the aerodynamic and aeroacoustic performance of airfoils, engineers are frustrated in making decisions on new blade designs. This is particularly true for small wind turbines, which operate at low Reynolds numbers where airfoil aerodynamic characteristics are both sensitive and difficult to predict. Thus, the present work must be considered in the context of the broader research effort that includes wind tunnel *aerodynamic* and *aeroacoustic* tests. The aerodynamic tests were conducted at the University of Illinois at Urbana-Champaign, and the aeroacoustic tests were conducted at the Netherlands National Aerospace Laboratory (NLR) in Emmeloord, Netherlands. The results, documented in NREL reports [1,2] and several papers in these conference proceedings, provide a valuable airfoil database for designers who wish to consider the tested airfoils.

For the acoustic tests described in this paper, the two-dimensional airfoil models were mounted between two acoustically treated endplates and tested with and without boundary layer trips and a turbulence grid, at three angles of attack and five wind tunnel speeds corresponding to Reynolds numbers from 0.2 to 1.0 million. Approximately 500 configurations were tested. Results were obtained in the form of 1/3-octave band acoustic "source plots" using conventional sum-and-delay beam forming, which allows separation of source and background noise. Further processing provided noise spectra and overall sound pressure[1] levels. The principal objective was to obtain a relative comparison of the prominent noise sources for the tested airfoils and conditions. Significant results are presented as a comparison of noise emissions for the various airfoils, the influence of inflow turbulence on leading-edge noise and the effect of boundary layer tripping. Because this paper is a significant condensation of the larger NREL report [2], many details have been omitted.

SOURCES OF AIRFOIL NOISE

There are six different sources that independently generate airfoil acoustic emissions [3,4]: inflow turbulence, turbulent boundary layer trailing edge interaction, separating flow, laminar boundary layer vortex shedding, trailing edge bluntness (von Karman) vortex shedding and tip vortex formation. These sources are superimposed to form the total noise spectrum from a wind turbine blade. The spectra are often summed to calculate an overall sound power[2] level.

Inflow turbulence noise caused by the interaction of the leading edge of an airfoil with a turbulent inflow is often called leading edge noise. Researchers currently think that sharp leading edge geometries are more susceptible to inflow turbulence noise.

The other sources of noise are collectively called airfoil self noise, because they are caused by the airfoil interacting with its own boundary layer and near wake. If the trailing edge thickness of the airfoil is very thin relative to the boundary layer thickness, as was the case for the models tested, there will be no trailing edge bluntness noise. And two-dimensional airfoil models tested between endplates do not have a tip vortex or any associated noise, although interaction between the endplate boundary layer and model-endplate juncture may cause extraneous noise.

Turbulent boundary layer trailing edge noise is generally considered to be the most important source of airfoil self noise for modern wind turbine blades. In this phenomenon, the unsteady pressure waves in the turbulent boundary layer are amplified and radiated by the

---

[1] Sound is characterized by small pressure fluctuations overlaying atmospheric pressure, but the human ear does not respond linearly to the amplitude of sound pressure [4]. Doubling the amplitude produces the sensation of louder noise, but it seems far less than twice as loud. For this reason, the scale used to characterize sound pressure amplitudes is logarithmic, which is an approximation of the actual response of the human ear. The definition of sound pressure level L_p is

$L_p = 10 \cdot \log [\underline{p}^2 \div \underline{p}^2_{ref}]$ expressed in decibels, dB,

where, $\underline{p}$ is the root mean square sound pressure and $\underline{p}_{ref}$ has a value of 20 μ Pa corresponding to the weakest audible sound – the threshold of human hearing – at a frequency of 1000 Hz.

A sound spectrum shows the distribution of acoustic energy as a function of frequency in either 1/3-octave or narrow bands. The overall sound pressure level represents the total acoustic energy, obtained by summing the spectral values over the whole frequency range.

[2] Whereas sound <u>pressure</u> level is a property of the observer location [4], the total strength of a source of sound is characterized by the sound <u>power</u> emitted by the source. In general, the sound power $\boldsymbol{P}$ transmitted through a surface $\boldsymbol{S}$ is the integral of the sound intensity $\boldsymbol{I}$ (energy transmitted per unit time and unit area) over the surface. If the surface $\boldsymbol{S}$ encloses the source of the sound, then $\boldsymbol{P}$ is the total sound power emitted by the source. The definition of sound power level is

$L_w = 10 \cdot \log [\boldsymbol{P} \div \boldsymbol{P}_{ref}]$ expressed in decibels, dB,

where $\boldsymbol{P}_{ref} = 10^{-12}$ watts is the standard reference sound power. The eardrum can detect incoming sound power as weak as one picowatt, and exposure to incoming sound power of more than one watt will result in some hearing loss.

sharp trailing edge. As the angle of attack increases, the thickness of the turbulent boundary layer increases and large-scale unsteady structures can dominate noise production from the trailing edge. For fully separated flow, noise can radiate from the entire chord.

Laminar boundary layer vortex shedding noise is created by a feedback loop between vortices being shed at the trailing edge and instability waves in the laminar boundary layer upstream. This source of noise can occur on either the suction or pressure side of the airfoil, and it can be particularly annoying because it is often manifested in pure tones that result from feedback amplification. It is not likely to be important for large turbines operating at high Reynolds number, but it may be significant for small wind turbines.

AIRFOIL MODELS

Tests were conducted on seven airfoil models, each having a 22.86 cm chord and a 0.51 m span. Six of the airfoils are either being used or considered for use on small wind turbine blades. These are the FX63-137, S822, S834, (Selig-Donovan) SD2030, (Selig-Giguere) SG6043 and (Selig-Hanley) SH3055. The models are shown in Figure 1 along with a NACA 0012 profile (center of photograph) used as a benchmark for comparison to previous results obtained by the National Aeronautics and Space Administration (NASA) [5].

The airfoil models were built to exacting tolerances, where the difference between the specified and as-built surface was required to be within 0.05% of the model chord, or 0.1143 mm. Trailing edge thickness was to be no greater than 0.375 mm with 0.1875 mm as a preferred upper limit. A coordinate measuring machine was used to verify the final dimensions, and in virtually every case, the model geometry was within the specified tolerances. Figure 2 shows a typical result. The noticeable deviation at the trailing edge is because the airfoil coordinates result in a trailing edge thickness of zero, which is impossible to fabricate.

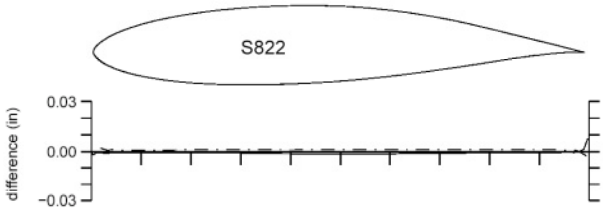

Figure 2. S822 airfoil model accuracy (difference between specified and measured coordinates)

The NACA 0012 model was constructed of carbon-fiber fabric pre-impregnated with epoxy resin and cured at room temperature. Although the accuracy of this model was acceptable, we decided to construct the remaining models of solid aluminum to accelerate the fabrication process.

The S822 model was also used to test micro electro mechanical systems (MEMS) tabs, which are being investigated for aerodynamic controls. These devices were mounted at 95% chord on the pressure side of the airfoil, using double-sided adhesive tape. Two sets of four MEMS were tested, comprising various tab heights and spacing. Although space limitations preclude reporting the test results in this paper, they are detailed in the NREL report [2].

For tests with a fully turbulent boundary layer, tripping was initiated using zigzag tape of width = 5% chord over the entire model span at 2% and 5% chord on the suction and pressure sides of the airfoil, respectively. The standard trip thickness was 0.25 mm, but for some conditions, trips of up to 0.5 mm were used. In some cases a stethoscope was employed to verify whether or not the trips induced the desired boundary layer transition. The stethoscope was attached to an L-shaped total-pressure tube, which was traversed manually over the surface of the model. Transition from a laminar to a turbulent boundary layer was observed by listening.

The geometric angle of attack (α) set in the wind tunnel was corrected [5] to account for flow curvature, resulting in an effective angle of attack (α_{eff}).

MEASUREMENTS AND DATA ANALYSES

The aeroacoustic tests were conducted in NLR's Small Anechoic Wind Tunnel KAT (Figure 3). This open circuit wind tunnel, the test section of which is surrounded by an anechoic room that is completely covered with foam wedges, yields more than 99% sound absorption above 500 Hz. Horizontal endplates are mounted to the upper and lower sides of a rectangular 0.38 m x 0.51 m nozzle, providing a semi-open test section for airfoil self noise measurements. To suppress reflections, the endplates are acoustically lined with layers of sound absorbing foam covered by perforated plates. For inflow turbulence measurements, a turbulence grid consisting of diagonally oriented, cylindrical 12 mm bars with a mesh width of 60 mm is installed in the nozzle. Although the tunnel is equipped with a force balance, that information was not used in these tests.

Test Section Calibration

To verify acceptable flow quality, a calibration study was performed using hot-wire anemometers in the empty test section. Cross hot-wires were used to measure the turbulence intensity and flow angularity with

and without the turbulence grid. Hot wire traverses were made in both cross flow directions for two Mach numbers, M=0.12 and M=0.18, at two axial locations roughly corresponding to the position of the leading and trailing edge of the tested models.

The test section calibration resulted in profiles of axial velocity, axial turbulence intensity, lateral turbulence intensity and flow angularity. Without the turbulence grid, the central part of the test section had turbulence levels of 1% or less. With the turbulence grid, the levels increased to 9% and 5% at locations corresponding to the model leading and trailing edges, respectively. Although the flow angularity increased slightly with increasing speed and turbulence level, it always remained within 1^o in the central area of the test section.

Microphone Array

Sound pressure level data were acquired using an acoustic array consisting of 48 ½-inch LinearX M51 microphones mounted in an open grid. Frequency dependent sensitivities of the individual microphones were taken from calibration sheets. No corrections were applied for microphone directivity, because this effect is the same for all airfoils and less than 2 dB for angles up to 45^o and frequencies up to 15 kHz. Phase matching of the microphones was checked prior to the test using a calibration source at a known position.

To obtain high resolution at low frequencies, the array dimensions needed to be rather large (0.8 m x 0.6 m^2). The microphone pattern was designed for maximum side lobe suppression at frequencies between 1 kHz and 20 kHz. The array was placed outside the tunnel flow 0.6 m from the tunnel axis, either on the suction or pressure side of the model as dictated by the test matrix. The relatively small distance between the array and the model was chosen to obtain a maximum signal-to-noise ratio. The center of the array was placed at the same height as the tunnel axis. Thus, the levels measured by the array represent airfoil noise levels radiated in the average direction of the array microphones. Because the source directivity for trailing edge and inflow turbulence noise is expected to be the same for all airfoils, the comparisons of noise from different airfoils is valid.

Acoustic data from the array microphones were synchronously measured at a sample frequency of 51.2 kHz and a measurement time of 30 s. A 500 Hz high-pass filter was used to enhance the dynamic range.

Test Program

Array measurements were made on the suction side of the six candidate airfoils, with and without tripping and turbulence grid for three angles of attack. The NACA 0012 airfoil was tested for the same conditions as in Reference 4: with and without trip, without turbulence grid, for four Reynolds numbers and five angles of attack. An overview of the suction-side test matrix is shown in Table 1. For a number of conditions, pressure side array measurements were also made to determine directivity effects. Some measurements were repeated with thicker zigzag tape to assess its effectiveness in tripping the boundary layer.

Data Processing

Processing methods and computer programs are referenced in the test report [2], but details are not discussed because of their proprietary nature.

Conventional sum-and-delay beam forming was applied to obtain acoustic source plots as illustrated in Figure 4. The effect of sound refraction by the tunnel shear layer was corrected using the Amiet method [6], and the array scan plane was placed in the plane of the model and rotated in accordance with the angle of attack. Using these source plots, noise originating from the model was separated from background noise.

A number of special measures were taken in the beamforming process. First, the main diagonal in the cross power matrix (auto powers) was discarded to suppress the influence of tunnel background noise. Second, a spatial window was applied to the microphone signals to reduce the effective array aperture with increasing frequency and reduce coherence loss effects.

For quantitative comparison of different airfoils and conditions, the array results were processed to obtain narrowband or 1/3-octave-band spectra for specific source regions (again, the main diagonal in the cross power matrix was discarded). The acoustic data were processed using a block size of 2048, yielding a narrowband frequency resolution of 25 Hz. By defining an integration contour around the mid-span of the model, extraneous noise sources at junctions of the model and end plates were suppressed. A preliminary review of the test results showed that for measurements without the turbulence grid, noise was radiated from the trailing edge of the model. Therefore, in those cases, the mid-span integration area was centered on the trailing edge. For measurements with the turbulence grid, the dominant noise source was observed to be located at the leading edge of the model. In those cases, the integration contour was centered on the leading edge. This process is illustrated in Figure 5.

Because the integration area cuts through the line source region at the leading or trailing edge, “leakage”

from sources outside the integration area into the integration contour, and vice versa, will occur. The magnitude of this effect depends on array resolution, and therefore on frequency. To account for this effect, a "line source correction" was applied using simulations similar to those described by Oerlemans and Sijtsma [7]. The resulting spectral levels are Sound Power Levels produced by 10 cm of span.

Extraneous Noise Sources

In some cases, the airfoil noise levels were so low that, despite the procedures described above, the spectra were dominated by extraneous wind tunnel noise sources. To facilitate rapid judgment of the validity of the measured levels, procedures were developed to indicate the importance of tunnel noise in the spectra.

For a significant number of conditions, the trailing edge noise levels were influenced by extraneous sources at the model-endplate junctions. These "corner sources" are illustrated in Figure 6. A routine was developed to determine the importance of these corner sources and, in cases where their influence on the trailing edge noise level is more than 1 dB, to calculate an upper limit for the trailing edge noise level. In graphs of the trailing edge noise spectra, these upper limits are indicated by the absence of a marker (symbol) at that specific frequency. If significant corner sources are absent, calculated noise levels are assumed to be absolute and a marker is placed at that specific frequency on the spectral plots. These data processing methods were successful in isolating the corner sources and mitigating their influence on calculated noise levels. Furthermore, a technique was identified for eliminating the corner sources entirely in future tests [2].

For measurements with the turbulence grid in place, background noise from the grid itself, rather than corner sources, often obscured the leading edge noise levels. In those cases, leading edge noise levels were compared to those obtained in the empty test section (with turbulence grid) for the same speed. If the leading edge noise level was at least 6 dB higher than the background noise level, a marker is placed at that specific frequency on the spectral plots. Absence of a marker indicates that the spectral level was influenced by grid noise.

RESULTS

A large amount of data was acquired and analyzed in the experiments, but only a small amount can be presented in this paper. The reader may wish to obtain the full NREL report [2], which includes graphical presentations and narrative discussion of the following topics:

- Test section calibration data
- Sound power level *trailing* edge noise spectra for the six small wind turbine airfoils tested, including the effect of boundary layer tripping
- Comparison of trailing edge noise data to benchmark NACA 0012 data [5]
- Sound power level *leading* edge noise spectra for the six small wind turbine airfoils tested, including the effect of boundary layer tripping
- Normalized leading and trailing edge noise spectra illustrating collapse of data for different speeds
- Emission of pure tones for several airfoils, including suppression by aggressive boundary layer trips,
- Directivity tests with the microphone array on both pressure and suction sides of the model
- Leading edge noise and trailing edge noise sound power level comparison for all airfoils at 32 m/s and several angles of attack
- Trailing edge noise spectra for various MEMS configurations tested on the S822 airfoil
- Discovery of techniques to significantly reduce extraneous corner source noise.

Trailing Edge Noise Spectra

Figure 7 illustrates typical trailing edge noise spectra obtained from acoustic source plots such as those shown in Figure 4. Results for the tripped boundary layer exhibit smooth broadband spectra typically associated with trailing edge noise. Results for the untripped boundary layer show some significant peaks that can be associated with laminar boundary layer vortex shedding [5]. The frequency of the peaks increases with speed at the angle of attack shown.

We investigated the directivity of trailing edge noise by conducting certain tests with the array first on the suction side and then on the pressure side. The directivity was found to be symmetrical about the chord, as demonstrated by Figure 8. Speed dependence, occurrence of tones, and comparison between different airfoils will be discussed in subsequent sections.

Leading Edge Noise Spectra

When the airfoils were tested with the turbulence grid installed in the tunnel, leading edge inflow turbulence noise became the dominant source for all airfoils. This was clearly indicated in the source plots (Figure 9), which reveal no prominent trailing edge emissions. The dynamic range of the source plots was 12 dB, which implies that the leading edge source was much greater than the trailing edge source. For the S822 airfoil at the same wind speed and angle of attack, the peak *leading* edge noise level (Figure 10) with the turbulence grid was around 90 dB compared to a peak

trailing edge noise level (Figure 7) of approximately 70 dB without the grid. With the turbulence grid, tripped and untripped results were identical, and leading edge noise directivity was found to be symmetrical around the chord.

It is important to note that the level of turbulence in the tunnel was much greater than is typically experienced in the atmosphere at typical rotor speeds. The literature does not provide any evidence that leading edge noise is a prominent source for large wind turbines, and conventional wisdom holds that trailing edge noise is dominant. NREL researchers are currently formulating an experimental approach to investigate this hypothesis.

Normalized Noise Spectra

To investigate the speed dependence of the airfoil noise levels, it is useful to normalize the noise spectra (Figure 11). Here, normalized sound power level, given by $PWL_{norm} = PWL - 10 \cdot \log(U^m)$; PWL is the airfoil sound power level determined from array measurements; the exponent m denotes the speed dependence of airfoil noise levels. Sound intensity p^2 is proportional to tunnel speed U^m, with p the acoustic pressure. PWL_{norm} is plotted against Strouhal number $St=f \cdot c/U$, where f is the acoustic frequency and c is the model chord. Typically, Strouhal scaling is based on boundary layer thickness, but because that information was not available, the model chord was used.

The best data collapse was obtained for a value of the exponent $m = 4.5$ determined iteratively. This is slightly lower than the value of 5 found in Reference 4. Some explanations are discussed in the full NREL report [2]. The S822 airfoil data in Figure 11 is provided for illustration, but review of the spectra for all airfoils showed very good data collapse for trailing edge noise in *tripped* conditions. For a given angle of attack, the trailing edge noise levels at different speeds coincided within 1-2 dB. Because normalization in terms of St and PWL_{norm} works well for the turbulent boundary layer trailing edge noise, experimental results for one speed can be extrapolated to other speeds.

For *untripped* conditions, peak Strouhal numbers for different speeds were found to coincide within about 30%. A slight increase in St with increasing speed suggests that a better collapse of peak frequencies could be obtained by using the boundary layer thickness as the length scale in St rather than chord, because boundary layer thickness at the trailing edge will decrease with increasing Reynolds number [5].

The spectral levels for the *untripped* results did not collapse as well as for the *tripped* data. Other values of the exponent m did not significantly improve the collapse. This illustrates that the normalization in terms of St and PWL_{norm} was not very successful for the complex feedback mechanism associated with laminar boundary layer vortex shedding noise, which is an important source for untripped airfoils at low Reynolds numbers.

We also normalized the leading edge (inflow turbulence) noise spectra in a manner similar to that described for trailing edge noise. The best collapse of data was obtained for the exponent $m = 6$, which is in good agreement with theoretical predictions for low frequency inflow turbulence noise [4]. Figure 12 provides an example for the S822 airfoil.

Comparison to Benchmark

Acoustic measurements on the NACA 0012 airfoil enabled direct comparison to benchmark data from NASA [5]. The tested airfoil shapes and chords were identical, and in both studies, the model was mounted between endplates attached to opposite sides of a rectangular tunnel nozzle. There were some differences in the manner of boundary layer tripping, but the NLR measurements were done at the same tunnel speeds and effective angles of attack as the NASA study.

Detailed comparisons of the test results are beyond the scope of this paper, but in general, the spectral characteristics (Figure 13) agreed quite well. Broadband spectra for the tripped cases and spectral humps (tones) for a number of untripped cases were reproduced. The *tripped* results revealed an interesting difference between the NASA and NLR data. Although the sound power levels compared quite well for intermediate frequencies, the NASA data consistently exhibited a hump around 1 kHz that did not appear in the NLR data. Possible explanations for this behavior are the topic of continuing dialogue among NLR, NASA, and NREL researchers. Issues include differences in the manner of boundary layer tripping (NASA trips were more severe) and differences in measurement technique (NASA used a 2-microphone correlation method and NLR used a 48-microphone array).

Pure Tones

One of the most interesting observations of the test campaign was the presence of intense, narrowband peaks in the trailing edge noise spectra for several airfoils at different operating conditions. These are called "pure tones" and are perceived as such by a listener. They are illustrated in Figure 14 for the trailing edge noise spectra of the untripped S834 (α=10°), SG6043 (α=0°) and SD2030 (α=0°) airfoils. The nature of these tones was investigated in more detail at 22.4 m/s, be-

cause they were most pronounced at this tunnel speed. The spectra for these cases show peaks at around 1 kHz and 2 kHz for all three airfoils. The angle of attack range for which these tones occurred was estimated by listening in the test section during a sweep of angle of attack. This gave the following ranges: $7.5° < \alpha < 13°$ for S834, $-8° < \alpha < 2°$ for SG 6043, and $-10° < \alpha < 4°$ for SD 2030.

Although such tones sometimes result from blunt trailing edge vortex shedding, the extremely thin trailing edges of the models made this unlikely. Calculations of the Strouhal number (*St)*, which is approximately 0.2 for von Karman vortex shedding, confirmed this was not the cause. We hypothesized, therefore, that laminar boundary layer vortex shedding caused the tones. To investigate this hypothesis, we applied a different thickness of zigzag tape and observed the effects. By tripping one side of the airfoil at a time, we could determine where the tones originated. For the S834 and SD2030 airfoils, it was the pressure side, whereas for the SG6043 airfoil, the tones originated from the suction side. Stethoscope measurements on the pressure side of the untripped S834 model indicated a laminar boundary layer up to about 80% chord. With tripping, transition to a turbulent boundary layer occurred directly behind the trip at 5% chord. This observation supported the hypothesis that the tones were due to laminar boundary layer vortex shedding.

The sensitivity of the tones to trip thickness was investigated in more detail for the S834 airfoil, with results shown in Figure 15. The untripped case (Figure 14) shows the narrowband peak at 925 Hz and the harmonic at 1850 Hz. It can be seen that the standard trip thickness of 0.25 mm on both sides of the airfoil was not effective. In fact, the level of the tones increased slightly with respect to the untripped case, and a harmonic appears at 2775 Hz. Application of a slightly thicker trip (0.30 mm) on the pressure side caused the spectral level to decrease dramatically and the 925 Hz and 1850 Hz tones to vanish completely. Interestingly, the broadband level decreases even further after the addition of a 0.30 mm trip on the suction side. While analysis of one case is not conclusive, this suggests that the suction side boundary layer dominates broadband noise production, whereas the pressure side may generate tones if it is not properly tripped.

Another interesting observation was that the tones disappeared in the presence of upstream turbulence. Observation of the source plots with and without the turbulence grid showed that the inflow turbulence removed the trailing edge tones, and the grid noise became dominant. Evidently, the inflow turbulence interrupts the feedback mechanism responsible for the tones.

Comparison of Airfoils

An important objective of the wind tunnel tests was to observe the noise levels of the different airfoils. All the models were not tested under identical conditions, but a common point for comparison does exist at 32 m/s and angles of attack of 0°, 10° and 18°. (The NACA 0012 data were taken at a slightly different speed of 31.7 m/s and angles of attack of 0°, 9.5° and 16.5°.)

The NREL report [2] compares the trailing edge noise spectra of the different airfoils. For the untripped condition, the noisiest airfoils were the SD 2030 and SG 6043 at 0° and the NACA 0012 and S834 at 10°. For the tripped condition, in which pure tones were largely eliminated, noise levels were reduced in virtually every case. Figure 16, in which tripped and untripped spectra are displayed side-by-side, shows this trend. Although the comparison among airfoils is obscured by the fact that for many frequencies only upper limits are available (see 'Extraneous Noise Sources' above), it appears that the FX63-137 and SH3055 airfoils are somewhat noisier than the others. These observations are reflected in Figure 17, which shows the A-weighted[3] overall sound power level obtained by summing the 1/3-octave band sound pressure levels between 0.8 kHz and 12.5 kHz. These overall sound power levels are an *upper limit* for the actual two-dimensional trailing-edge noise.

We also compared the inflow turbulence noise spectra for the airfoils. Because the results were virtually identical for tripped and untripped conditions, only tripped data were examined. Differences in leading edge noise of 8 dB were observed between the quietest and noisiest airfoils. By examining these results in relationship to the airfoil shapes, we observed a general trend—the sharper the airfoil leading edge, the higher the inflow turbulence noise. This trend is demonstrated in Figure 18, which plots the A-weighted overall noise levels for three angles of attack. These were obtained by summing the 1/3-octave band levels between 1 kHz and 2.5 kHz where airfoil noise is attributed to inflow turbulence. Data in Figure 18 are presented from left to right in the order of decreasing airfoil leading edge radius.

It is important to note that comparing airfoil noise data at the same angle of attack can be misleading, because

[3] The ear is not equally sensitive to tones of different frequencies. Maximum response occurs between 2 kHz and 3 kHz, where the hearing threshold is somewhat less than 0 dB. A 100 Hz tone, however, must have an intensity of 40 dB to be heard [4]. Therefore, weighted sound levels have been introduced where lower frequencies are de-emphasized in a manner similar to human hearing. A-weighting is most commonly used and is well suited for sound levels that are not too high.

the airfoils may operate at different angles of attack. For example, peak aerodynamic efficiency for the FX63-137 occurs around $\alpha = 4^o$ while the S822 is best around $\alpha = 8^o$ [1]. Therefore, to estimate which airfoil will be quieter, we must compare at their respective design points (angle of attack, Reynolds number, surface condition, and tip speed). Following this logic, Figure 17 suggests that the FX63-137 ($\alpha_{eff}=4.4^o$, $\alpha=10^o$) is likely to be quieter than the S822 ($\alpha_{eff}=7.9^o$, $\alpha=18^o$). However, inspection of the S822 trailing edge noise spectra in Figure 16 shows a sharp peak between 1 kHz and 2 kHz, indicating laminar boundary layer vortex shedding and a boundary layer that was not fully tripped. This shows that simply comparing data at the same Reynolds number is not sufficient. The *character* of the boundary layer, in particular the extent of laminar flow, must also be simulated. In fact, the data showed [2] that the FX63-137 and S822 with their boundary layers fully tripped had no tones and suggested that the S822 was really quieter than the FX63-137.

SUMMARY

Large amounts of high quality data were obtained for the airfoils tested in this project. This is attributed to precise models and rigorous, mature test methods. One consequence of this precision was that trailing edge bluntness vortex shedding noise did not materialize owing to the extremely thin trailing edge of the models. We believe model precision also contributed to the good agreement obtained for the spectral characteristics of the NACA0012 airfoil tested at NASA and compared to the NLR results, although a discrepancy in sound power level at 1 kHz is still being investigated.

In quiescent inflow, trailing edge noise is dominant. Test results suggest that untripped airfoils operating at low Reynolds numbers (< 1 million) can be expected to exhibit pure tones at some angles of attack. For example, it was common to observe tones of 10 dB – 15 dB above the broadband level. This was attributed to laminar boundary layer vortex shedding. It was also observed that proper tripping eliminated pure tones and reduced broadband noise. Even those airfoils that did not exhibit pure tones experienced a reduction in sound power level of up to 3 dB(A) when tripped. In highly turbulent inflow, pure tones disappeared, probably due to the suppression of the laminar boundary layer and/or disruption of the feedback mechanism responsible for laminar boundary layer vortex shedding noise.

The tested airfoils exhibited notably different turbulent boundary layer trailing edge noise levels. This source, which is likely to be dominant for typical wind turbines, differed by as much as 8 dB(A) among the airfoils tested. Leading edge inflow turbulence noise becomes the dominant source, masking trailing edge noise, in the presence of severe upstream turbulence. There appears to be a trend of increasing inflow turbulence noise with increasing airfoil leading edge sharpness.[4]

In considering the noise of different airfoils, it may not be appropriate to compare at the same angle of attack. It is more important to compare at the angle of attack expected at the design condition, which may vary significantly from one airfoil to another.

ACKNOWLEDGEMENTS

A lengthy and ambitious project such as this has many contributors. In our case, credit must first be given to the extraordinary craftsmanship of Yvan Tinel of Northbrook, Illinois, who fabricated the airfoil models to exacting specifications. Michael Selig of the University of Illinois at Urbana-Champaign performed the coordinate measurements and plotting. The test engineers and technicians at NLR deserve special mention. They operate a superb facility and exhibit great professionalism and a commitment to quality.

REFERENCES

[1] Selig, M. and McGranahan, B., 2003, *Wind Tunnel Aerodynamic Tests of Six Airfoils for Use on Small Wind Turbines*, NREL SR-500-34515.

[2] Oerlemans, S., 2003, *Wind Tunnel Aeroacoustic Tests of Six Airfoils for Use on Small Wind Turbines*, NREL SR-500-34470.

[3] Moriarty, P. and Migliore, P, 2003, *Semi-empirical Aeroacoustic Noise Prediction Code for Wind Turbines*, NREL TP-500-34478.

[4] Wagner, S., Bareiß, R. and Guidati, G, 1996, Wind Turbine Noise, Springer-Verlag, Berlin, pp. 14-21.

[5] Brooks, T., Pope, D. and Marcolini, M., 1989, *Airfoil Self-Noise and Prediction*, NASA Reference Publication 1218.

[6] Amiet, R., 1978, "Refraction of Sound by a Shear Layer," *Journal of Sound and Vibration*, Vol. 58, No. 2, pp 467-482.

[7] Oerlemans and Sijtsma, 2002, "Determination of Absolute Levels from Phased Array Measurements Using Spatial Source Coherence," AIAA-2002-2464.

[4] The turbulence intensity in the NLR tests was greater than anticipated in the atmosphere because of differences in mean velocity between tunnel speeds and typical blade tip speeds. Although evidence is not seen in the literature, researchers generally agree that leading edge noise is not significant for typical large wind turbines. This may not be true for small turbines having thin airfoils with sharp leading edges, especially downwind rotors operating in a tower wake.

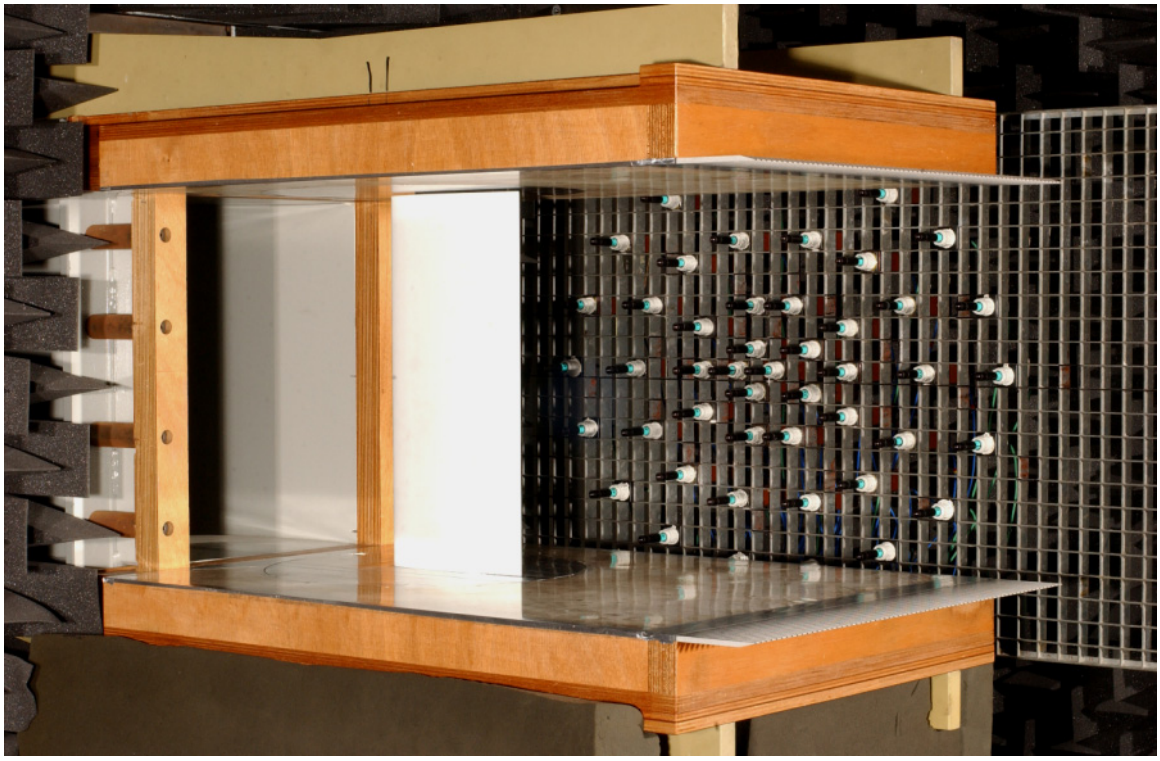

Figure 3. NLR anechoic wind tunnel set up with acoustically lined endplates and microphone array

	Turbulence grid off		Turbulence grid on	
Airfoil	**Trip**	**No trip**	**Trip**	**No trip**
S822	0.20/ 0.35/ 0.50/ 0.75/ 1.0	0.20/ 0.35/ 0.50/ 0.75/ 1.0	0.20/ 0.35/ 0.50/ 0.75/ 1.0	0.20/ 0.35/ 0.50/ 0.75/ 1.0
S834	0.20/ 0.35/ 0.50/ 0.75	0.20/ 0.35/ 0.50/ 0.75	0.20/ 0.35/ 0.50/ 0.75	0.20/ 0.35/ 0.50/ 0.75
FX 63-137	0.20/ 0.35/ 0.50/ 0.75	0.20/ 0.35/ 0.50/ 0.75	0.20/ 0.35/ 0.50/ 0.75	0.20/ 0.35/ 0.50/ 0.75
SG 6043	0.11/ 0.20/ 0.35/ 0.50	0.11/ 0.20/ 0.35/ 0.50	0.11/ 0.20/ 0.35/ 0.50	0.5
SH 3055	0.50/ 0.75/ 1.0	0.50/ 0.75/ 1.0	0.50/ 1.0	0.50/ 1.0
SD 2030	0.20/ 0.35/ 0.50	0.20/ 0.35/ 0.50	0.20/ 0.50	0.20/ 0.50
NACA0012	0.50/ 0.62/ 0.87/ 1.12	0.50/ 0.62/ 0.87/ 1.12	0.50/ 0.62/ 0.87/ 1.12	0.50/ 0.62/ 0.87/ 1.12

Table 1. Test matrix showing measured Reynolds numbers (in millions) with the array on the suction side of the model. For the six small-wind-turbine airfoils, all Reynolds numbers were tested at geometrical angles of attack of 0°, 10° and 18°, except the shaded boxes (0°, 5° and 10°). The NACA 0012 airfoil was tested at geometrical angles of attack of 0°, 4.5°, 9.0°, 12.0° and 16.5°, to obtain the same effective angles of attack (0°, 2°, 4°, 5.3° and 7.3°) as in Reference 2 (0°, 2°, 4°, 5.3° and 7.3°).

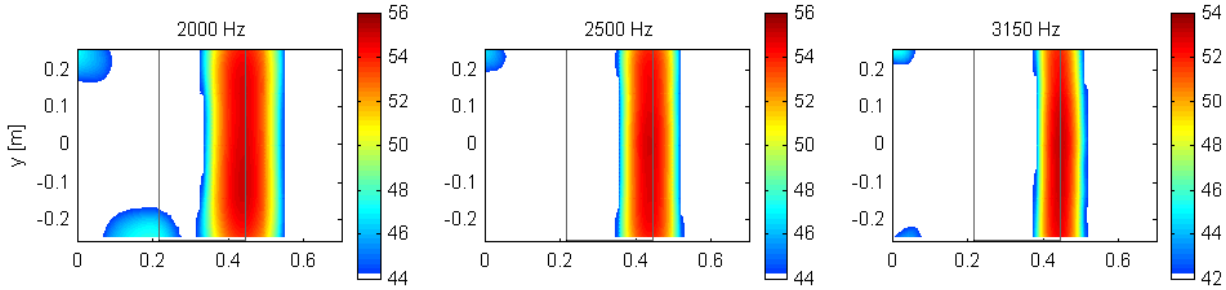

Figure 4. Acoustic source plots for the untripped NACA 0012 airfoil at 39.6 m/s and α=0° (array on pressure side) illustrating prominent trailing-edge emissions. Flow direction is from left to right.

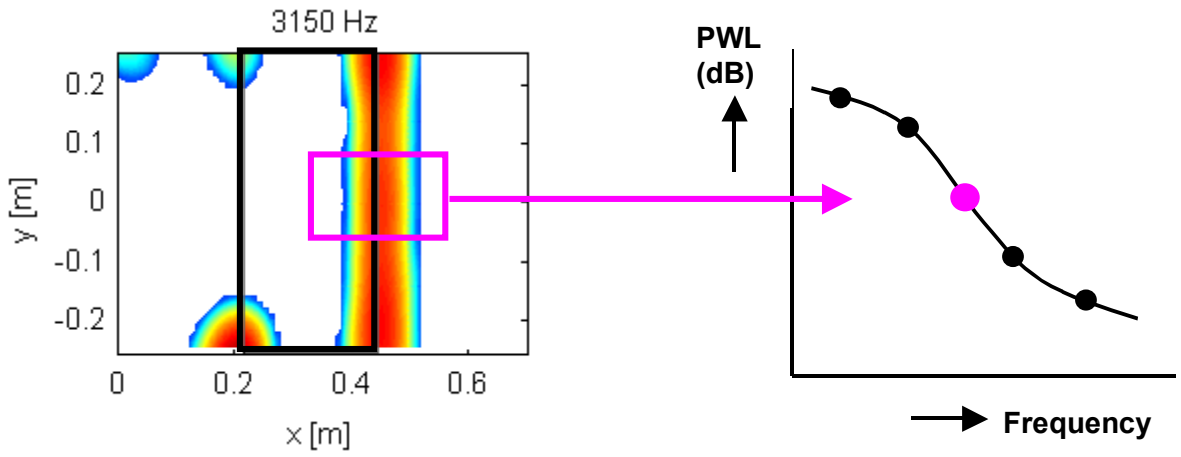

Figure 5: Acoustic source plot (left) indicating noise source locations in the plane of the model. The model contour is indicated by the (black) vertical rectangle: flow goes from left to right. The (pink) horizontal rectangle indicates the trailing edge integration contour used to translate acoustic source plots to airfoil noise spectra. For measurements with the turbulence grid, a leading edge integration contour was used.

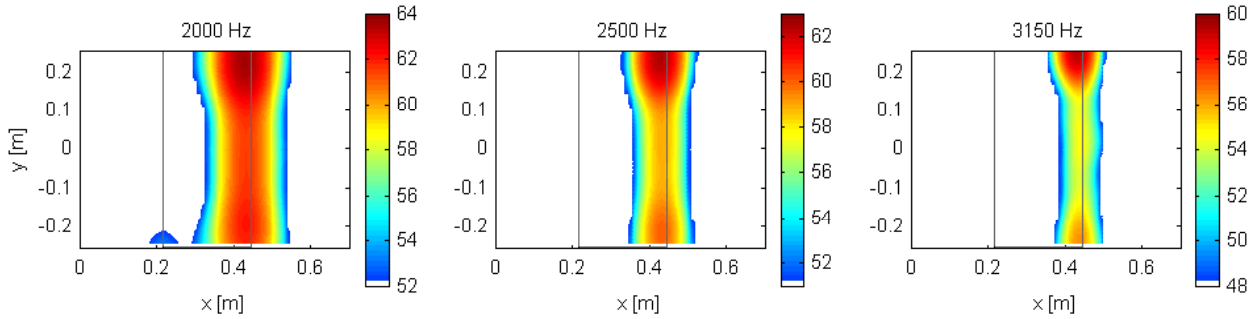

Figure 6: Acoustic source plots for tripped S822 airfoil at 47.9 m/s and α=0° (array on suction side). Note the extraneous "corner sources" in contrast to the uniform sources shown in Figure 4.

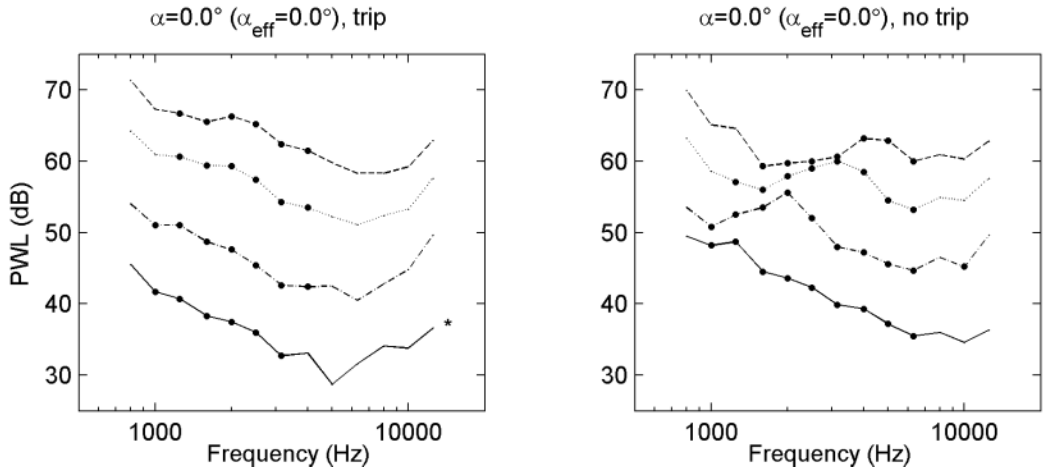

*Figure 7. Trailing edge noise spectra for the S822 airfoil (array on suction side) plotted versus frequency in Hz. __ 22.4 m/s; _._ 32.0 m/s; … 47.9 m/s; _ _ 63.9 m/s. * indicates a trip thickness of 0.5 mm.*

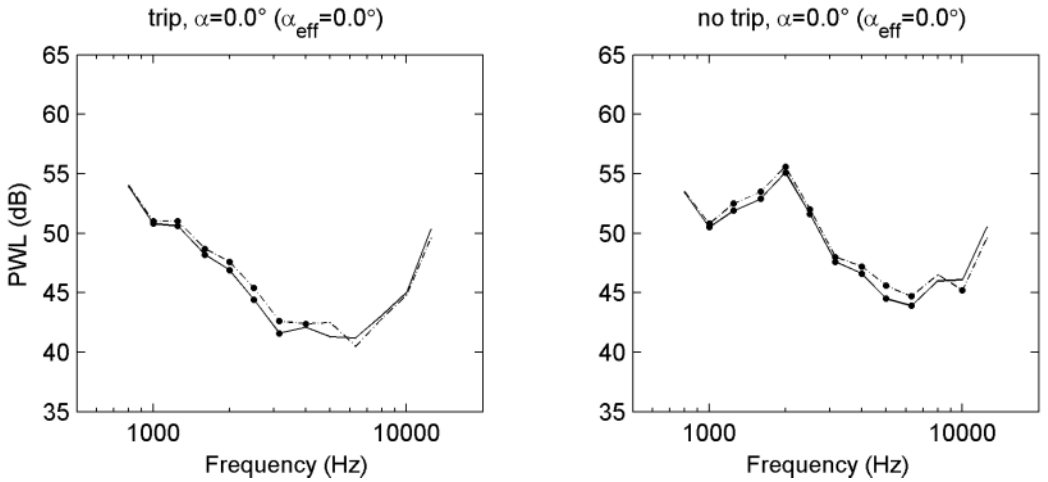

Figure 8. Trailing edge noise spectra for S822 airfoil at 32 m/s. __ array on pressure side; _._ array on suction side. Note the symmetry about the chord, suggesting uniform directivity.

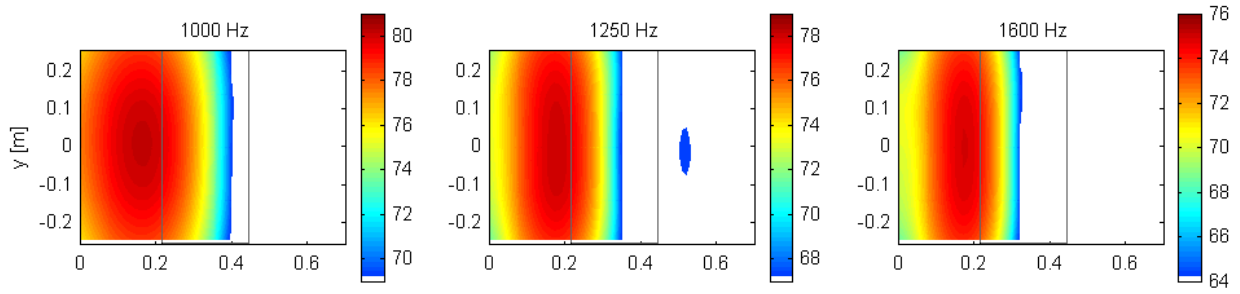

Figure 9. Leading edge noise from SD 2030 airfoil with trip, with turbulence grid, at a tunnel speed of 32.0 m/s and α=18° (array on suction side). Note the dominance of the leading edge sources.

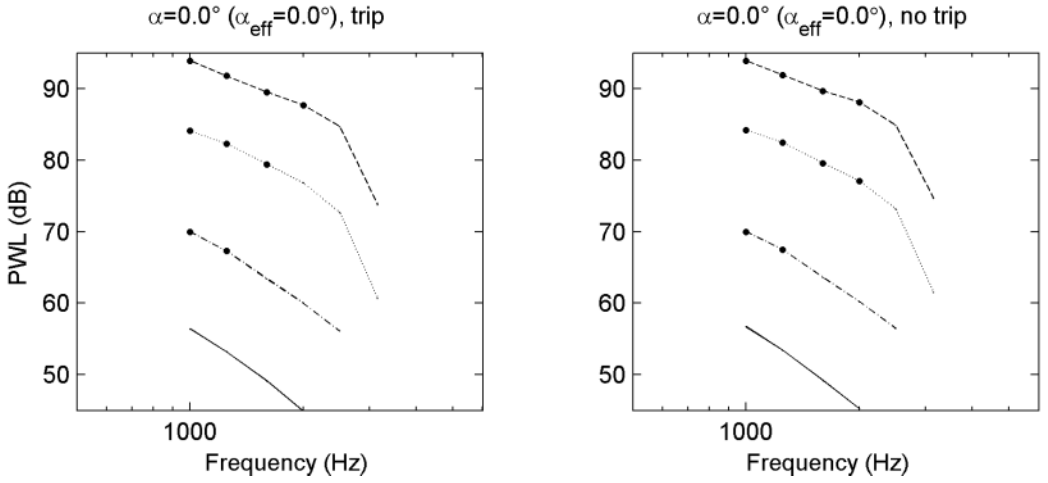

Figure 10. Leading edge noise spectra for S822 airfoil (array on suction side). __ 22.4 m/s; _._ 32.0 m/s; … 47.9 m/s; _ _ 63.9 m/s. Note that the levels are much higher than the trailing edge noise spectra shown in Figure 7.

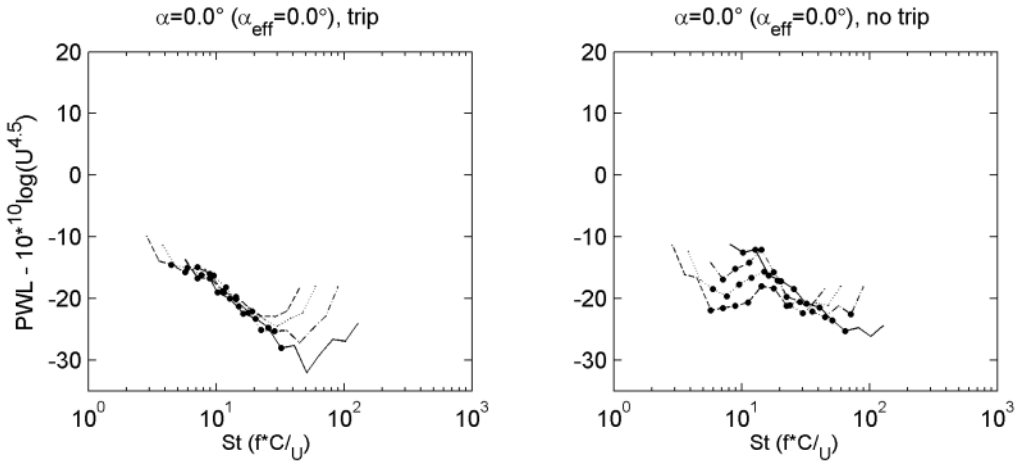

Figure 11. Normalized trailing edge noise spectra for the S822 airfoil (array on suction side) plotted versus Strouhal number, St = f · c ÷ U. __ 22.4 m/s; _.._ 32.0 m/s; … 47.9 m/s; _ _ 63.9 m/s.

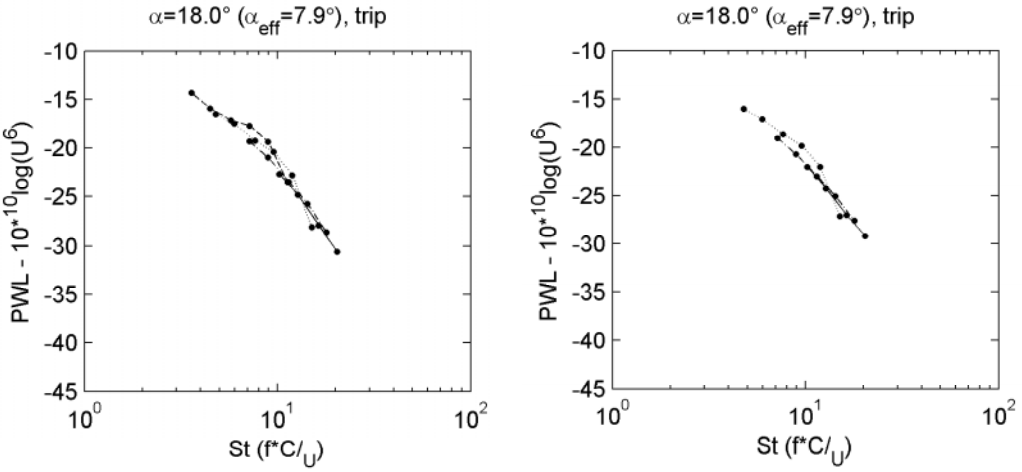

Figure 12. Normalized inflow-turbulence noise spectra for tripped S822 (left) and S834 (right) airfoils (array on suction side). __ 22.4 m/s; _.._ 32.0 m/s; … 47.9 m/s; _ _ 63.9 m/s.

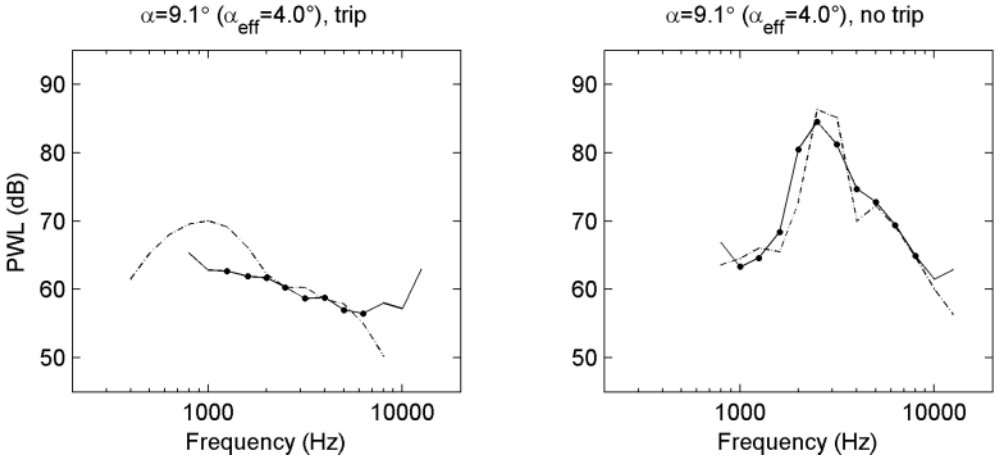

Figure 13. Trailing edge noise spectra for the NACA 0012 airfoil at 55.5 m/s. __ NLR data (array on suction side); _.._ NASA data [4].

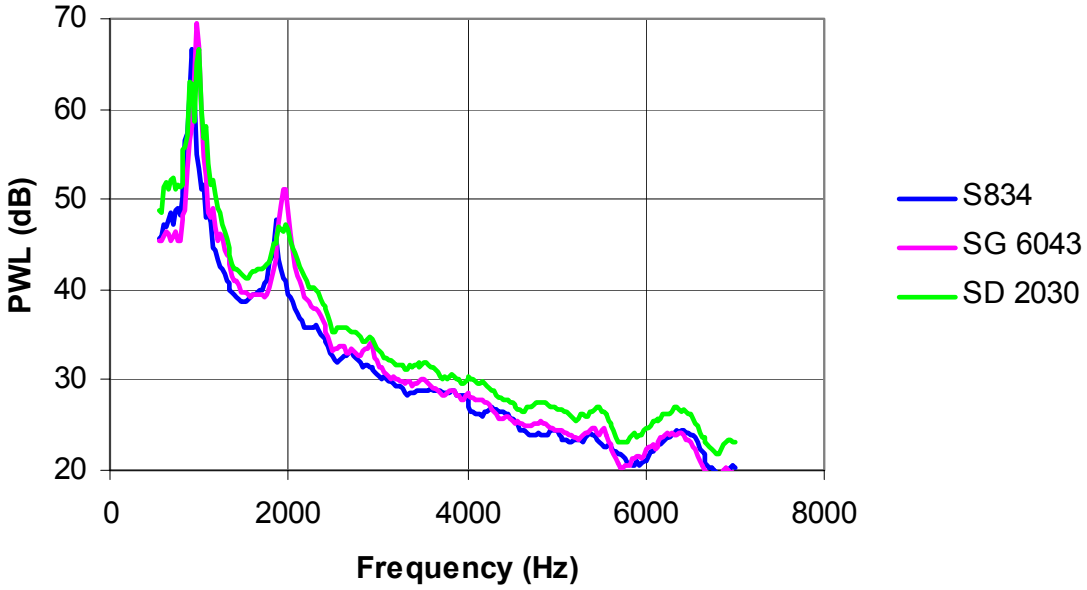

Figure 14. Narrowband trailing edge noise spectra for three untripped airfoils that showed intense tones (U=22.4 m/s; α=10° for S834, α=0° for SG 6043 and SD 2030).

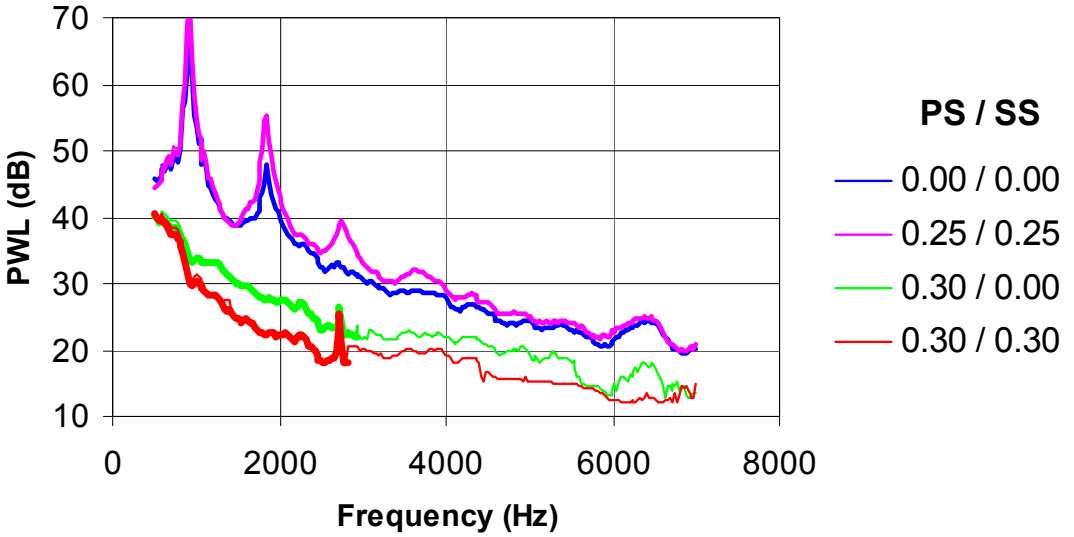

Figure 15. Narrowband trailing edge noise spectra for S834 airfoil at 22.4 m/s and α=10° as a function of trip thickness on pressure side (PS) and suction side (SS). A thin line indicates that these spectral values are an upper limit for the trailing-edge noise level.

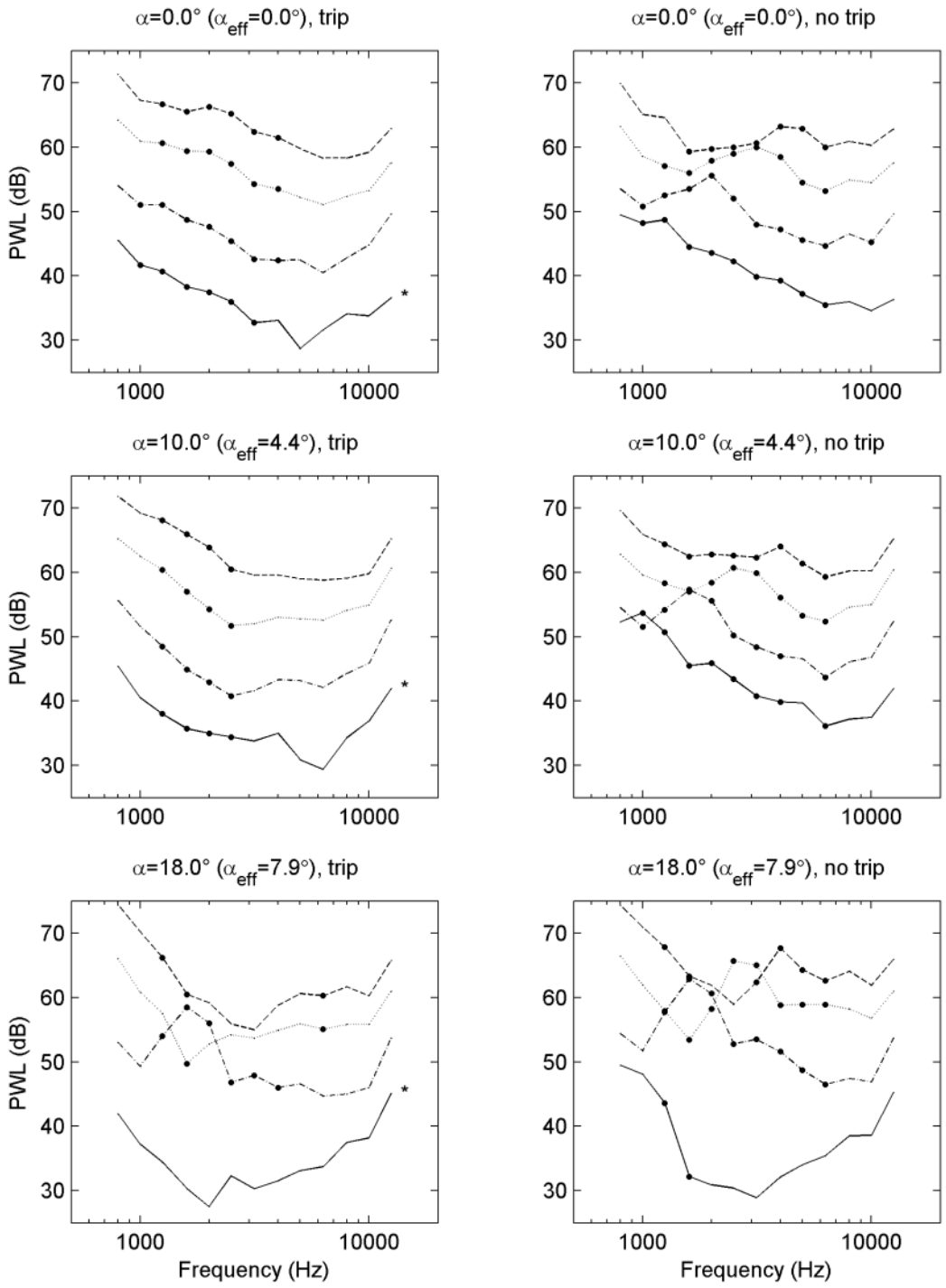

*Figure 16. Trailing edge noise spectra for S822 airfoil (array on suction side). __ 22.4 m/s; _._ 32.0 m/s; … 47.9 m/s; _ _ 63.9 m/s. * indicates a trip thickness of 0.5 mm.*

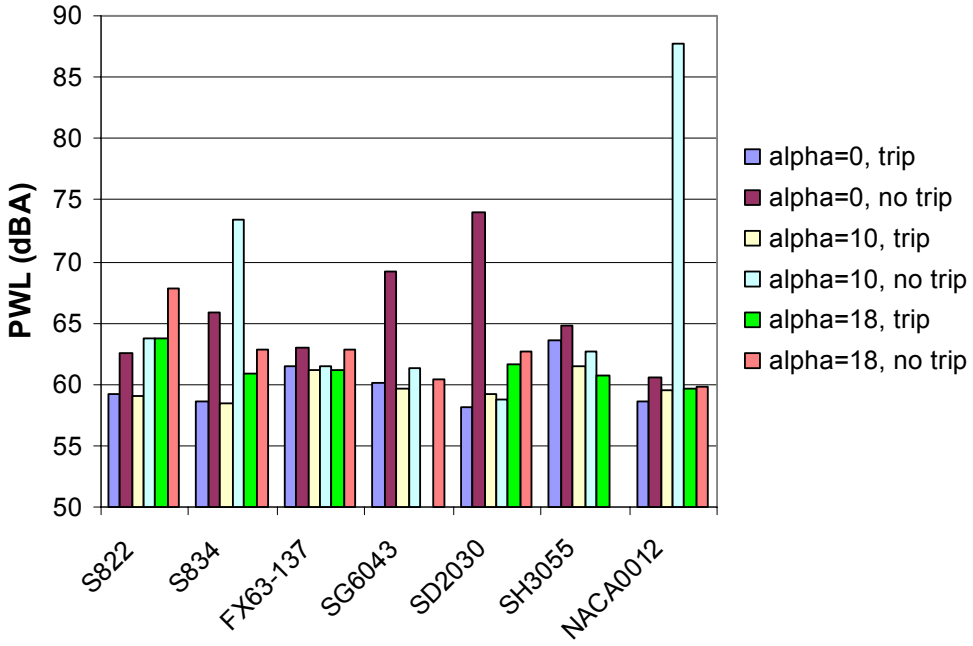

Figure 17. A-weighted overall trailing edge noise levels at 32 m/s.

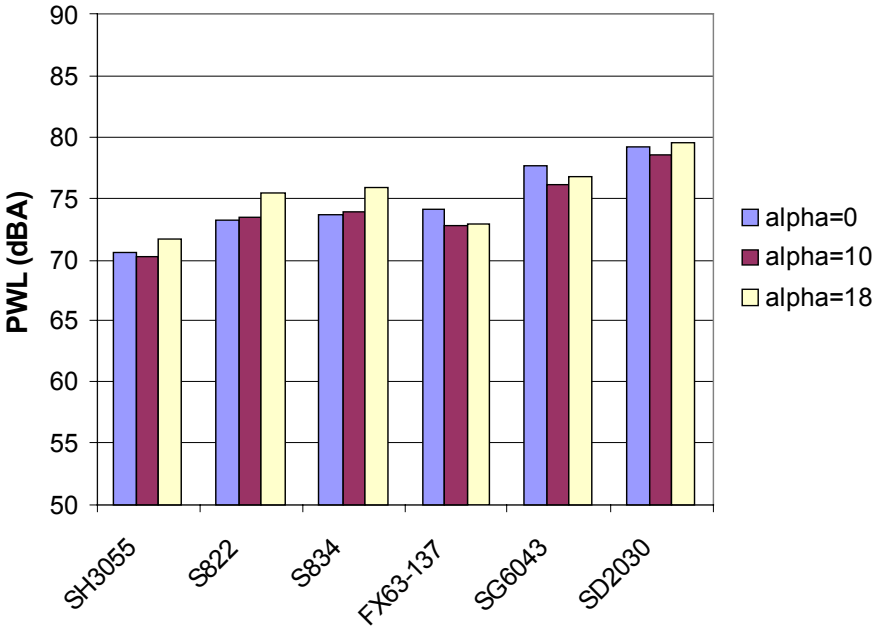

Figure 18. A-weighted overall leading edge noise levels at 32 m/s. Airfoils are presented from left to right in the order of decreasing leading edge radius and increasing leading edge inflow turbulence noise.

REPORT DOCUMENTATION PAGE

Form Approved
OMB NO. 0704-0188

1. AGENCY USE ONLY (Leave blank)	2. REPORT DATE	3. REPORT TYPE AND DATES COVERED
	December 2003	Conference paper

4. TITLE AND SUBTITLE
Wind Tunnel Aeroacoustic Tests of Six Airfoils for Use on Small Wind Turbines: Preprint

5. FUNDING NUMBERS
WER3.1830

6. AUTHOR(S)
P. Migliore and S. Oerlemans

7. PERFORMING ORGANIZATION NAME(S) AND ADDRESS(ES)
National Renewable Energy Laboratory
1617 Cole Blvd.
Golden, CO 80401-3393

8. PERFORMING ORGANIZATION REPORT NUMBER
NREL/CP-500-35090

9. SPONSORING/MONITORING AGENCY NAME(S) AND ADDRESS(ES)

10. SPONSORING/MONITORING AGENCY REPORT NUMBER

11. SUPPLEMENTARY NOTES

12a. DISTRIBUTION/AVAILABILITY STATEMENT
National Technical Information Service
U.S. Department of Commerce
5285 Port Royal Road
Springfield, VA 22161

12b. DISTRIBUTION CODE

13. ABSTRACT *(Maximum 200 words)*
Aeroacoustic tests of seven airfoils were performed in an open jet anechoic wind tunnel. Six of the airfoils are candidates for use on small wind turbines operating at low Reynolds number. One airfoil was tested for comparison to benchmark data. Tests were conducted with and without boundary layer tripping. In some cases a turbulence grid was placed upstream in the test section to investigate inflow turbulence noise. An array of 48 microphones was used to locate noise sources and separate airfoil noise from extraneous tunnel noise. Trailing edge noise was dominant for all airfoils in clean tunnel flow. With the boundary layer untripped, several airfoils exhibited pure tones that disappeared after proper tripping was applied. In the presence of inflow turbulence, leading edge noise was dominant for all airfoils.

14. SUBJECT TERMS
airfoils; small wind turbines; aeroacoustic tests

15. NUMBER OF PAGES

16. PRICE CODE

17. SECURITY CLASSIFICATION OF REPORT	18. SECURITY CLASSIFICATION OF THIS PAGE	19. SECURITY CLASSIFICATION OF ABSTRACT	20. LIMITATION OF ABSTRACT
Unclassified	Unclassified	Unclassified	UL